752 Chem. Mater. 1991, 3, 752-758

Transition Metals Complexed to Ordered Mesophases.[1] Synthesis, Mesomorphic Behavior, and EPR Investigations on a Homologous Series of *N*-(4-Alkoxysalicylidene)-4′-alkylanilines Complexed to Copper(II)

Mauro Ghedini* and Stefania Morrone

Dipartimento di Chimica, Università della Calabria, I-87030 Arcavacata (CS), Italy

Dante Gatteschi and Claudia Zanchini

Dipartimento di Chimica, Università di Firenze, I-50144 Firenze, Italy

Received January 10, 1991. Revised Manuscript Received May 23, 1991

The synthesis, mesomorphic properties, and EPR characterization of a homologous series of *N*-(4-(dodecyloxy)salicylidene)-4′-alkylanilines complexed to copper(II) are reported. These copper mesogens are microcrystalline solids at room temperature that upon heating or cooling down from the isotropic liquid display at least a smectic A phase. The EPR spectra, recorded at room temperature and after heating the samples to the clearing points, give results that are in agreement with the molecular packings previously proposed on the basis of X-ray investigations and shows that the smectic A phase gives rise to a peculiar EPR line shape.

Introduction

The match between the mesogenic nature of appropriate molecules and the peculiar properties associated to a transition metal has been recently considered as a promising strategy for the preparation of new anisotropic materials. The metallomesogens so obtained form a novel, wide class of liquid crystals for which suitable synthetic strategies are developed in conjunction with the investigation of their physical properties.[2]

We are currently investigating two different series of metallomesogens, namely, organometallic palladium(II) complexes[1,3] and copper(II) coordination compounds.[4] The latter belong to a class of paramagnetic metallomesogens comprising other copper(II) species[4-19] as well as vanadyl,[6,7,20] lutetium,[21] nickel,[22,23] and iron(III)[24] compounds.

The present paper deals with the preparation, thermotropic properties and EPR investigations of the homologous series of copper(II) complexes $(R_nL)_2Cu$ arising from the Schiff bases, R_nLH, of general formula shown in Chart I. The members of such a series, where R_n is CH_3, C_2H_5, C_3H_7, or C_4H_9, are mesogenic compounds whose mesomorphic properties (see Table II) have been recently investigated by X-ray diffraction.[25] The $(C_4H_9L)_2Cu$ complex, in the S_A mesophase, was found to consist in a two-dimensional array of interdigitated molecules (with periodicities along the *b* and *c* axis of 8.60 and 30.22 Å, respectively, Scheme I).[26] A further Cu···Cu correlation at 3.85 Å was found by EXAFS measurements.[27]

We report here the detailed synthetic pathways of these materials, together with the EPR investigation performed on the complexes with the R_n aliphatic chain ranging from CH_3 to C_8H_{17}.

Chart I. General Formula of the R_nLH Schiff Bases

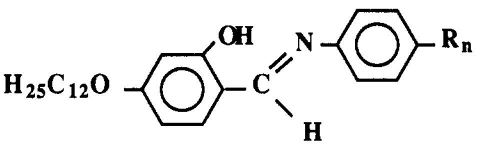

R_n= CH_3 C_2H_5 C_3H_7
C_4H_9 C_6H_{13} OC_6H_{13}
C_8H_{17}

Scheme I. Sketch of the Molecular Array Displayed by the $(C_4H_9L)_2Cu$ S_A Phase in a (100) Plane (*b* = 8.60 Å; *c* = 30.22 Å)

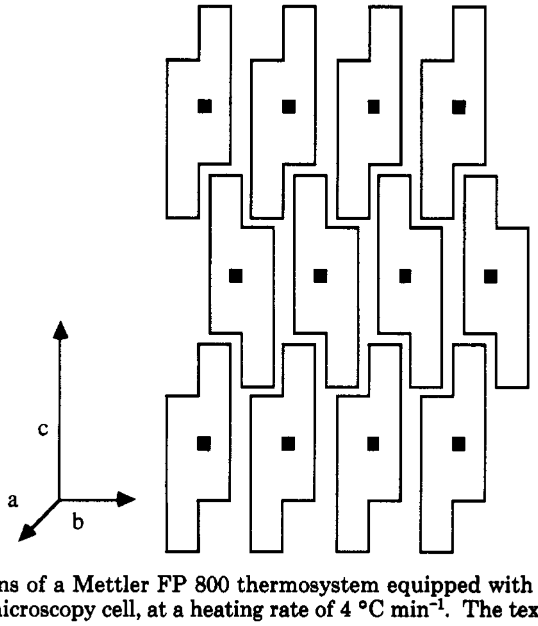

Experimental Section

General Procedures. The ^1H NMR spectra ($CDCl_3$, standard $SiMe_4$) were recorded on a Bruker AW 80 spectrometer; the IR spectra (KBr pellets) were performed on a Perkin-Elmer 1330 spectrometer. Elemental analyses were obtained from the Microanalysis Laboratory of the Dipartimento di Chimica, Università della Calabria, Italy. The thermal behavior was monitored by means of a Mettler FP 800 thermosystem equipped with a FP 84 microscopy cell, at a heating rate of 4 °C min^{-1}. The textures

---

* To whom correspondence should be addressed.

(1) Part 9. Part 8: Ghedini, M.; Morrone, S.; De Munno, G.; Crispini, A. *J. Organomet. Chem.*, in press.

(2) Giroud-Godquin, A. M.; Maitlis, P. M. *Angew, Chem., Int. Ed. Engl.* **1991**, *30*, 375.

0897-4756/91/2803-0752$02.50/0

of the various mesophases were observed by means of a Zeiss axioscope polarizing microscope equipped for photography and with a Linkam CO 600 heating stage.

EPR Measurements. The EPR spectra of the Schiff bases series $(R_nL)_2Cu$ were recorded at X-band frequency with a Bruker E-200 spectrometer in the temperature range −153 to 177 °C. The Q-band EPR spectra were obtained at room temperature with a Varian E-9 spectrometer.

The FORTRAN program used allows stimulation of the EPR spectra of polycristalline or glassy material for $S = {}^1/_2$ without restriction about the nuclear spin, using the spin Hamiltonian

$$\mathbf{H} = \mathbf{B} \cdot \mathbf{g} \cdot \mathbf{S} + \mathbf{I} \cdot \mathbf{A} \cdot \mathbf{S}$$

Simpson integration was used for the orientation on Θ and Φ angles,[28] both ranging from 0° to 180°. Both isotropic and anisotropic line widths and Gaussian and Lorentzian line shapes are allowed.

Chart II. Molecular Structure of the $(R_nL)_2Cu$ Derivatives

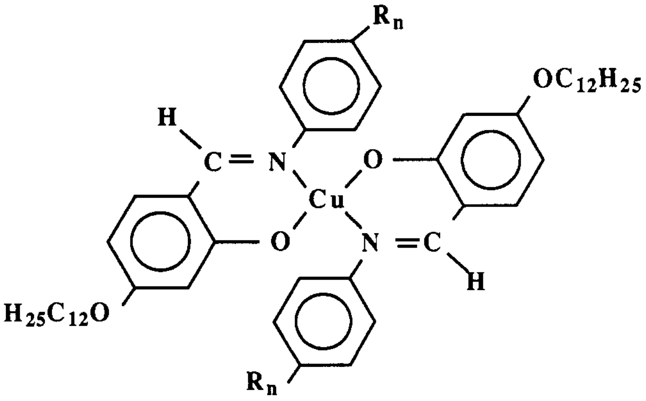

$R_n = CH_3$ C_2H_5 C_3H_7
C_4H_9 C_6H_{13} OC_6H_{13}
C_8H_{17}

The spectra were fitted by using six independent parameters, namely, the three g values and the total line width for each of them. No hyperfine was included because it is always merged in the line width. When more than one species appears to be present in different percentages, the computed spectrum is given by the sum of the contributions coming from each of them.

Synthesis of the Ligands. The synthesis of the R_nLH ligand were carried out under a nitrogen atmosphere. The standard chemicals, 2,4-dihydroxybenzaldehyde, 1-bromododecane, and the 4-substituted anilines, were used as supplied (Aldrich Chemical Co.).

The R_nLH preparations were performed from 2-hydroxy-4-(*n*-dodecyloxy)benzaldehyde and the appropriate 4-substituted anilines.

Preparation of 2-Hydroxy-4-(*n*-dodecyloxy)benzaldehyde. To a solution of 2,4-dihydroxybenzaldehyde (5.387 g, 39 mmol) in ethanol (30 mL) were added an ethanolic solution (30 mL) of potassium hydroxyde (2.184 g, 39 mmol) and 1-bromododecane (9.364 mL, 39 mmol). The resulting mixture, stirred under reflux for 5 h, produced a pale yellow precipitate (potassium bromide), which was filtered, and a yellow solution from which after removal of the solvent under reduced pressure a yellow oil forms. The oil was purified by cromatogratography (SiO_2) eluting with a mixture of diethyl ether and petroleum ether (v/v, 1/1). Evaporation of the solvent gave the product as a pale yellow oil, yield 11.050 g (95%). ^1H NMR (80 MHz, $CDCl_3$) δ 4.0 (t, 2 H, J = 5 Hz, $-OCH_2-$).

Preparations. CH_3LH. 2-Hydroxy-4-(*n*-dodecyloxy)benzaldehyde (0.980 g, 3.2 mmol) and 4-methylaniline (0.343 g, 3.2 mmol) were mixed in ethanol (10 mL) and stirred under reflux for 2 h. The color became yellow. The yellow precipitate that forms on cooling was filtered off, washed with cold pentane, and vacuum dried, yield 0.437g (35%). ^1H NMR (80 MHz, $CDCl_3$) δ 8.4 (s, 1 H, $-CH{=}N-$), 3.9 (t, 2 H, J = 5 Hz, $-OCH_2-$), 2.3 (s, 3 H, $-C_6H_4CH_3$). All the analogous R_nLH compounds were prepared as described for CH_3LH. Yields and selected ^1H NMR data (80 MHz, $CDCl_3$) are as follows:

C_2H_5LH. Yield, 45%. ^1H NMR δ 8.4 (s, 1 H, $-CH{=}N-$), 3.9 (t, 2 H, J = 5 Hz, $-OCH_2-$), 2.6 (q, 2 H, J = 5 Hz, $-C_6H_4CH_2-$).

C_3H_7LH. Yield, 59%. ^1H NMR δ 8.4 (s, 1 H, $-CH{=}N-$), 4.0 (t, 2 H, J = 5 Hz, $-OCH_2-$), 2.6 (t, 2 H, J = 5 Hz, $-C_6H_4CH_2-$),

C_4H_9LH. Yield, 49%. ^1H NMR δ 8.4 (s, 1 H, $-CH{=}N-$), 3.9 (t, 2 H, J = 5 Hz, $-OCH_2-$), 2.3 (t, 2 H, J = 5 Hz, $-C_6H_4CH_2-$).

$C_6H_{13}LH$. Yield, 40%. ^1H NMR δ 8.4 (s, 1 H, $-CH{=}N-$), 3.9 (t, 2 H, J = 5 Hz, $-OCH_2-$), 2.5 (t, 2 H, J = 5 Hz, $-C_6H_4CH_2-$).

$C_6H_{13}OLH$. Yield, 42%. ^1H NMR δ 8.4 (s, 1 H, $-CH{=}N-$), 3.9 (t, 4 H, J = 5 Hz, $-OCH_2-$).

$C_8H_{17}LH$. Yield, 43%. ^1H NMR δ 8.4 (s, 1 H, $-CH{=}N-$), 3.9 (t, 2 H, J = 5 Hz, $-OCH_2-$), 2.5 (t, 2 H, J = 5 Hz, $-C_6H_4CH_2-$).

Synthesis of the Complexes. Preparation of $(CH_3L)_2Cu$, 1. To a suspension of CH_3LH (198 mg, 0.5 mmol) in ethanol (10 mL) stirred at room temperature were added potassium hydroxyde (2.8 mg, 0.5 mmol) in ethanol (2 mL) and copper(II) acetate

---

(3) Ghedini, M.; Pucci, D.; De Munno, D.; Viterbo, D.; Neve, F.; Armentano, S. *Chem. Mater.* **1991**, *3*, 65.

(4) (a) Ghedini, M.; Armentano, S.; Bartolino, R.; Torquati, G.; Rustichelli, F. *Solid State Commun.* **1987**, *64*, 1191. (b) Ghedini, M.; Armentano, S.; Bartolino, R.; Kirov, N.; Petrov, M.; Nenova, S. *J. Mol. Liq.* **1988**, *38*, 207.

(5) Blazaut, B.; Barthon, C.; Tercier, N.; Andrè, J. J.; Simon, J. *J. Am. Chem. Soc.* **1987**, *109*, 6193 and references therein.

(6) Galyametdinov, Yu. G.; Bikchantaev, I. G.; Ovchinnikov, I. V. *Zh. Obshch. Khim.* **1988**, *58*, 1326 and references therein.

(7) (a) Serrano, J. L.; Romero, P.; Marcos, M.; Alonso, P. J. *J. Chem. Soc., Chem. Commun.* **1990**, 859. (b) Alonso, P. J.; Sanjuân, M. L.; Romero, P.; Marcos, M.; Serrano, J. L. *J. Phys.: Condens. Matter* **1990**, *2*, 9173.

(8) Paschke, R.; Zascke, H.; Maedicke, A.; Chipperfield, J. R.; Blake, A. B.; Nelson, P. G.; Gray, G. W. *Mol. Cryst. Liq. Cryst., Lett. Sect.* **1988**, *6*, 81.

(9) Muhlberger, B.; Haase, W. *Liq. Cryst.* **1989**, *5*, 251.

(10) Shaffer, T. D.; Shoth, K. A. *Mol. Cryst. Liq. Cryst.* **1989**, *93*, 8105.

(11) (a) Abied, H.; Guillon, D.; Skoulios, A.; Weber, P.; Giroud-Godquin, A. M.; Marchon, J. C. *Liq. Cryst.* **1987**, *2*, 269. (b) Giroud-Godquin, A. M.; Maldivi, P.; Marchon, J. C.; Beé, M; Carpentier, L. *Mol. Phys.* **1989**, *68*, 1353 and references therein.

(12) Van der Pol, J. F.; Neeleman, E.; Zwikker, J. W.; Molte, R. J. M.; Arenth, W.; Aerts, J.; Visser, R.; Picken, S. J. *Liq. Cryst.* **1989**, *6*, 577.

(13) (a) Marcos, M.; Romero, P.; Serrano, J. L.; Barberâ, J.; Levelut, A. M. *Liq. Cryst.* **1990**, *7*, 251. (b) Marcos, M.; Oriol, L.; Serrano, J. L.; Alonso, P. J.; Puèrtolas, J. A. *Macromolecules* **1990**, *23*, 5187.

(14) (a) Ohta, K.; Ema, H.; Yamamoto, I.; Matsuzaki, K. *Liq. Cryst.* **1988**, *3*, 1671. (b) Ohta, K.; Kasebe, H.; Ema, H.; Fujimoto, T.; Yamamoto, I. *J. Chem. Soc., Chem. Commun.* **1989**, 1610. (c) Ohta, K.; Takenaka, H.; Hasebe, Y.; Morizumi, T.; Fujimoto, T.; Yamamoto, I. *Mol. Cryst. Liq. Cryst.* **1991**, *195*, 103.

(15) (a) Chandrasekhar, S.; Sadashiva, B.; Sri Kanta, B. S. *Mol. Cryst. Liq. Cryst.* **1987**, *151*, 93. (b) Usha, K.; Vijayan, K.; Sadashiva, B. K.; Rao, P. R. *Mol. Cryst. Liq. Cryst.* **1990**, *185*, 1.

(16) Attard, G. S.; Cublum, P. R. *Liq. Cryst.* **1990**, *8*, 299.

(17) Hoshino, M.; Murakami, H.; Matsumaza, Y.; Inabe, T.; Maruyama, *Inorg. Chem.* **1990**, *29*, 1177.

(18) Bui, E.; Bayle, J. P.; Perez, F.; Liebert, L.; Courtieu, J. *Liq. Cryst.* **1990**, *8*, 513.

(19) Caruso, U.; Roviello, A.; Sirigu, A. *Liq. Cryst.* **1990**, *7*, 421, 431 and references therein.

(20) Galyametdinov, Yu. G.; Ivanova, O. I.; Ovchinnikov, I. V. *Zh. Obshch. Khim.* **1984**, *54*, 2796.

(21) Belarbi, Z.; Sirlin, C.; Simon, J.; Andre, J. J. *J. Phys. Chem.* **1989**, *93*, 8105 and references therein.

(22) Ohta, K.; Ema, H.; Morizumi, Y.; Watanabe, T.; Fujimoto, T.; Yamamoto, I. *Liq. Cryst.* **1990**, *8*, 311 and references therein.

(23) (a) Marcos, M.; Romero, P.; Serrano, J. L. *J. Chem. Soc., Chem. Commun.* **1989**, 1641. (b) Marcos, M.; Romero, P.; Serrano, J. L. *Chem. Mater.* **1990**, *2*, 495.

(24) Galyametdinov, Yu. G.; Ivanova, G. I.; Ovchinnikov, I. V. *Izv. Akad. Nauk. SSSR, Ser. Khim.* **1989**, 1931.

(25) Torquati, G.; Francescangeli, O.; Ghedini, M.; Armentano, S.; Nicoletta, F. P.; Bartolino, R. *Il Nuovo Cimento* **1990**, *12D*, 1363.

(26) Levelut, A. M.; Ghedini, M.; Bartolino, R.; Nicoletta, F. P.; Rustichelli, F. *J. Phys. (France)* **1989**, *50*, 113.

(27) Albertini, G.; Guido, A.; Mancini, G.; Stizza, S.; Ghedini, M.; Bartolino, R.; *Europhys. Lett.* **1990**, *12*, 629.

(28) Yokoi, H.; Addison, A. W. *Inorg. Chem.* **1977**, *16*, 1341.

Table I. Thermal Behavior for the R_nLH Compounds

compd	transn temp (°C) and mesophases[a]
R_1LH[b]	$K \xrightleftharpoons[66\ ^\circ C]{78\ ^\circ C} N \xrightleftharpoons{83\ ^\circ C} I$
R_2LH[b]	$K_2 \xrightarrow{59\ ^\circ C} S_A \xrightarrow{60\ ^\circ C} K_1 \xrightarrow{63\ ^\circ C} N \xrightleftharpoons{78\ ^\circ C} I$ $N \xrightarrow[60\ ^\circ C]{} S_A \xrightarrow[47\ ^\circ C]{} K_1$
R_3LH[b]	$K \xrightleftharpoons[39\ ^\circ C]{50\ ^\circ C} S_{A'} \xrightleftharpoons{63\ ^\circ C} S_A \xrightleftharpoons{72\ ^\circ C} N \xrightleftharpoons{85\ ^\circ C} I$
R_4LH[b]	$K_1 \xrightarrow{46\ ^\circ C} S_C \xrightarrow{60\ ^\circ C} S_{A'} \xrightleftharpoons{75\ ^\circ C} S_A \xrightleftharpoons{86\ ^\circ C} I$ $S_{A'} \xrightarrow{40\ ^\circ C} K_2$
R_6LH[c]	$K \xrightleftharpoons{51\ ^\circ C} S_C \xrightleftharpoons{90\ ^\circ C} S_A \xrightleftharpoons{95\ ^\circ C} I$
R_6OLH[c]	$K \xrightleftharpoons{74\ ^\circ C} S_C \xrightleftharpoons{105\ ^\circ C} S_A \xrightleftharpoons{122\ ^\circ C} I$
R_8LH[c]	$K \xrightleftharpoons{45^\circ C} S_C \xrightleftharpoons{93^\circ C} S_A \xrightleftharpoons{101^\circ C} I$

[a] K = crystal; N = nematic; S = smectic; I = isotropic liquid. [b] From ref 25. [c] Determined by optical microscopy.

Table II. Thermal Behavior for the $(R_nL)_2Cu$ Complexes

compd	transn temp (°C) and mesophases[a]
1[b]	$K_2 \xrightarrow{92\ ^\circ C} K_1 \xrightarrow{126\ ^\circ C} I$ $I \xrightarrow{104\ ^\circ C} S_A \xrightarrow[100\ ^\circ C]{} K_1$
2[b]	$K_2 \xrightarrow{81\ ^\circ C} K_1 \xrightarrow{128\ ^\circ C} I$ $I \xrightarrow{128\ ^\circ C} S_A \xrightarrow[117\ ^\circ C]{} K_1$
3[b]	$K_2 \xrightarrow{89\ ^\circ C} K_1 \xrightarrow{112\ ^\circ C} S_A \xrightleftharpoons[148\ ^\circ C]{152\ ^\circ C} I$ $S_A \xrightarrow[108\ ^\circ C]{} K_2$
4[c]	$K \xrightarrow{90^\circ C} S_E \xrightleftharpoons{98^\circ C} S_B \xrightleftharpoons{114^\circ C} S_A \xrightleftharpoons{140^\circ C} I$
5[d]	$K \xrightleftharpoons{119\ ^\circ C} S_A \xrightleftharpoons{140\ ^\circ C} I$
6[d]	$K \xrightleftharpoons{125\ ^\circ C} S_E \xrightleftharpoons{136\ ^\circ C} S_A \xrightleftharpoons{159\ ^\circ C} I$
7[d]	$K \xrightleftharpoons{121^\circ C} S_A \xrightleftharpoons{136^\circ C} I$

[a] K = crystal; N = nematic; S = smectic; I = isotropic liquid. [b] From ref 25. Determined by X-ray technique. [c] From ref 26. Determined by X-ray technique. [d] Determined by optical microscopy.

dihydrate (49 mg, 0.25 mmol). The mixture was stirred at room temperature for 4 h; the greenish solid formed in that time was filtered and recrystallized from chloroform–ethanol, yield 209 mg (81%). Anal. Calcd for $C_{52}H_{72}N_2O_4Cu$: C, 71.74; H, 8.34; N, 3.22. Found: C, 71.70; H, 7.96; N, 3.21.

The homologous $(R_nL)_2Cu$ complexes were synthesized following the procedure described for $(CH_3L)_2Cu$. Colors, yields, and analytical data are as follows:

$(C_2H_5L)_2Cu$, 2. Brown, yield 52%. Anal. Calcd for $C_{54}H_{76}N_2O_4Cu$: C, 73.64; H, 8.70; N, 3.18. Found: C, 74.18; H, 8.98; N, 3.23.

$(C_3H_7L)_2Cu$, 3. Brown, yield 54%. Anal. Calcd for $C_{56}H_{80}N_2O_4Cu$: C, 74.01; H, 8.87; N, 3.08. Found: C, 75.78; H, 9.18; N, 2.74.

$(C_4H_9L)_2Cu$, 4. Brown, yield 46%. Anal. Calcd for $C_{58}H_{84}N_2O_4Cu$: C, 74.36; H, 9.04; N, 2.99. Found: C, 73.93; H, 8.82; N, 2.78.

$(C_6H_{13}L)_2Cu$, 5. Greenish, yield 57%. Anal. Calcd for $C_{62}H_{92}N_2O_4Cu{\cdot}H_2O$: C, 73.66; H, 9.17; N, 2.77. Found: C, 73.75; H, 9.41; N, 2.74.

$(C_6H_{13}OL)_2Cu$, 6. Brown, yield 75%. Anal. Calcd for $C_{62}H_{92}N_2O_6Cu$: C, 72.80 H, 9.06; N, 2.74. Found: C, 73.36; H, 9.50; N, 3.00.

$(C_8H_{17}L)_2Cu$, 7. Greenish, yield 62%. Anal. Calcd for $C_{66}H_{100}N_2O_4Cu{\cdot}H_2O$: C, 76.29; H, 9.70; N, 2.69. Found: C, 76.28; H, 9.87; N, 2.68.

Results

Synthesis of the Compounds. The ligands were prepared in a two-step process. First, 2,4-dihydroxybenzaldehyde was reacted with *n*-dodecyl bromide, and the 2-hydroxy-4-(*n*-dodecyloxy)benzaldehyde so formed gave the R_nLH Schiff bases by treatment with the appropriate 4-R_n-aniline.

The R_nLH ligands react with $Cu(CH_3COO)_2{\cdot}2H_2O$, 2:1 molar ratio, affording brown or greenish solids, complexes 1–7, whose elemental analysis (Experimental Section) agree with the expected $(R_nL)_2Cu$ stoichiometry. A number of copper(II) Schiff base derivatives like 1–7 have been structurally characterized; therefore, by analogy with the literature data,[29,30] for all the present compounds we suggest the molecular geometry sketched in Chart II.

Mesomorphism. The R_nLH species are liquid crystals that display nematic and/or smectic mesophases (Table I). Moreover they form a homologous series (Chart I) of calamitic mesogens[31] that show the trend usually observed for transition temperatures and texture of the mesophases in similar series.[32]

Two molecules of the R_nLH ligands react with a copper(II) cation yielding the $(R_nL)_2Cu$ complexes, which keep an elongated molecular shape, whose geometry (Chart II) can be roughly assimilated with that of the R_nLH parents.

The compounds 1–7 are microcrystalline solids at room temperature that upon heating, for 3–7, or cooling from the isotropic liquid, for 1 and 2, display at least a smectic phase (Table II).

Remarkably, such a phase is the only one present, even for the complexes (1–3) obtained from the ligands having also a nematic mesophase (CH_3LH–C_3H_7LH in Table I). Moreover, a smectic A phase[33] is exhibited by the whole series 1–7, and further and more ordered smectic textures are shown by 4 and 6.

An account of the X-ray analysis performed on the CH_3LH–C_4H_9LH and 1–4 compounds has been previously given.[25] As reported in Table II, the mesomorphism concerning 4 is the richest; however, it should be pointed out that the S_E and S_B mesophases were recognized through X-ray techniques.[25] By contrast, the complexes 5–7 were simply investigated by optical microscopy; therefore, for such species the presence of further, undetected, smectic phases cannot be excluded.

EPR Investigation. Variable-temperature EPR spectra were recorded for all the $(R_nL)_2Cu$ compounds. The most interesting behaviors were observed for $(C_4H_9L)_2Cu$, 4, and $(C_6H_{13}L)_2Cu$, 5, whose thermal behavior will be described in detail.

$(C_4H_9L)_2Cu$, 4. The room-temperature X-band EPR spectrum of the freshly prepared compound appears to be

---

(29) Holm, R. H.; O'Connor, M. J. *Prog. Inorg. Chem.* **1971**, *14*, 328.

(30) Roviello, A.; Sirigu, A.; Iannelli, P.; Immirzi, A. *Liq. Cryst.* **1988**, *3*, 115.

(31) Beguin, A.; Billard, J.; Bonamy, F.; Buisine, J. M.; Cuvelier, P.; Dubois, J. C.; Le Barry, P. *Mol. Cryst. Liq. Cryst.* **1984**, *115*, 1.

(32) Kelker, H.; Hatz, R. *Handbook of Liquid Crystals*; Verlag Chemie: Weinheim, Germany, 1980.

(33) Demus, D.; Richter, L. *Texture of Liquid Crystals*; Verlag Chemie: Weinheim, Germany, 1978.

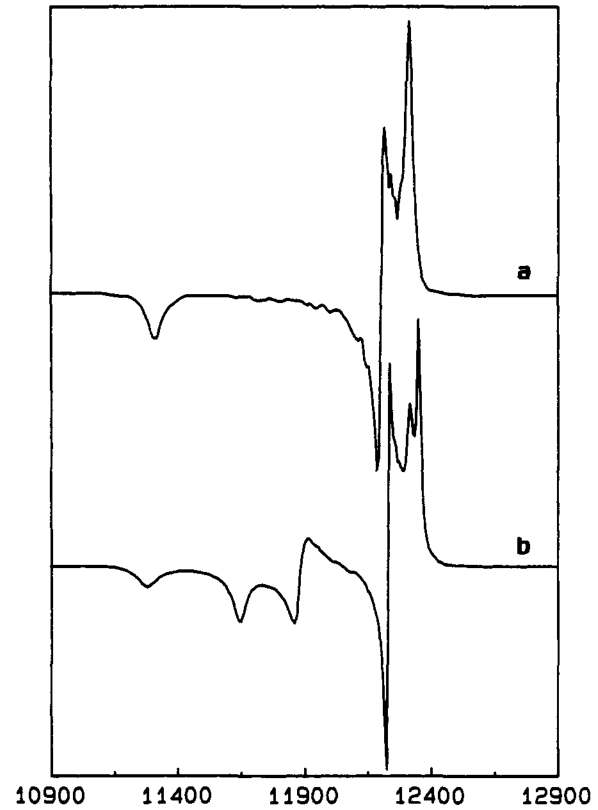

Figure 1. Room-temperature Q-band EPR spectra of freshly prepared samples of (a) $(C_4H_9L)_2Cu$, **4**, and (b) $(C_6H_{13}L)_2Cu$, **5**.

the superposition of two distinct spectra. The dominant one is axial with $g_\parallel \approx 2.22$ and $g_\perp = 2.05$. A weak feature at $g = 2.11$ was also observed. The room-temperature Q-band spectrum shown in Figure 1a evidences a small rhombicity of the main spectrum with $g_1 = 2.22$, $g_2 = 2.06$, and $g_3 = 2.04$ and shows a feature at $g = 2.11$.

After increasing the temperature the spectrum broadens up to 90 °C (observed smectic S_E phase) and to 98 °C (observed smectic S_B phase) and then narrows up to 114 °C (observed smectic S_A phase), where the EPR spectrum shows an asymmetric feature. The EPR spectra recorded for the three smectic phases are reported in Figure 2A.

The spectra recorded for the smectic S_A phases observed for $(C_2H_5L)_2Cu$, **2**, and $(C_3H_7L)_2Cu$, **3**, complexes are very similar to that of the S_A phase of **4**. The spectra of **4** remains substantially unchanged up to the melting point (140 °C) where the compound gives an isotropic pattern with $g_{av} = 2.09$. After cooling down to the melting point the spectrum changes, with $g_\parallel = 2.12$ and $g_\perp = 2.06$. Going back to room temperature, an increase in anisotropy is observed in a very broad spectrum with $g_\parallel = 2.26$ and $g_\perp = 2.06$. The spectra recorded at lower temperature are similar to those at room temperature of the freshly prepared compounds, showing an increase in the line width but no evidence of two different species.

$(C_6H_{13}L)_2Cu$, 5. The room-temperature X-band EPR spectrum of the freshly prepared compound is shown in Figure 3Aa and is given by the superposition of two distinct spectral series indicated with A and B.

The Q-band spectra shows six features with $g_1{}^A = 2.23$, $g_2{}^A = 2.06$, $g_3{}^A = 2.04$ and $g_1{}^B = 2.16$, $g_2{}^B = 2.11$, $g_3{}^B = 2.04$ as shown in Figure 1b. However, if the attribution of $g_1{}^A$, $g_1{}^B$, $g_2{}^B$ is sure, the attribution of the lowest g values to the two spectra is tentative.

The spectrum of the B species exhibits a temperature-dependent line width, and at 50 °C it is so broad that it practically disappears, whereas the spectrum A remains unchanged (see Figure 3Ab).

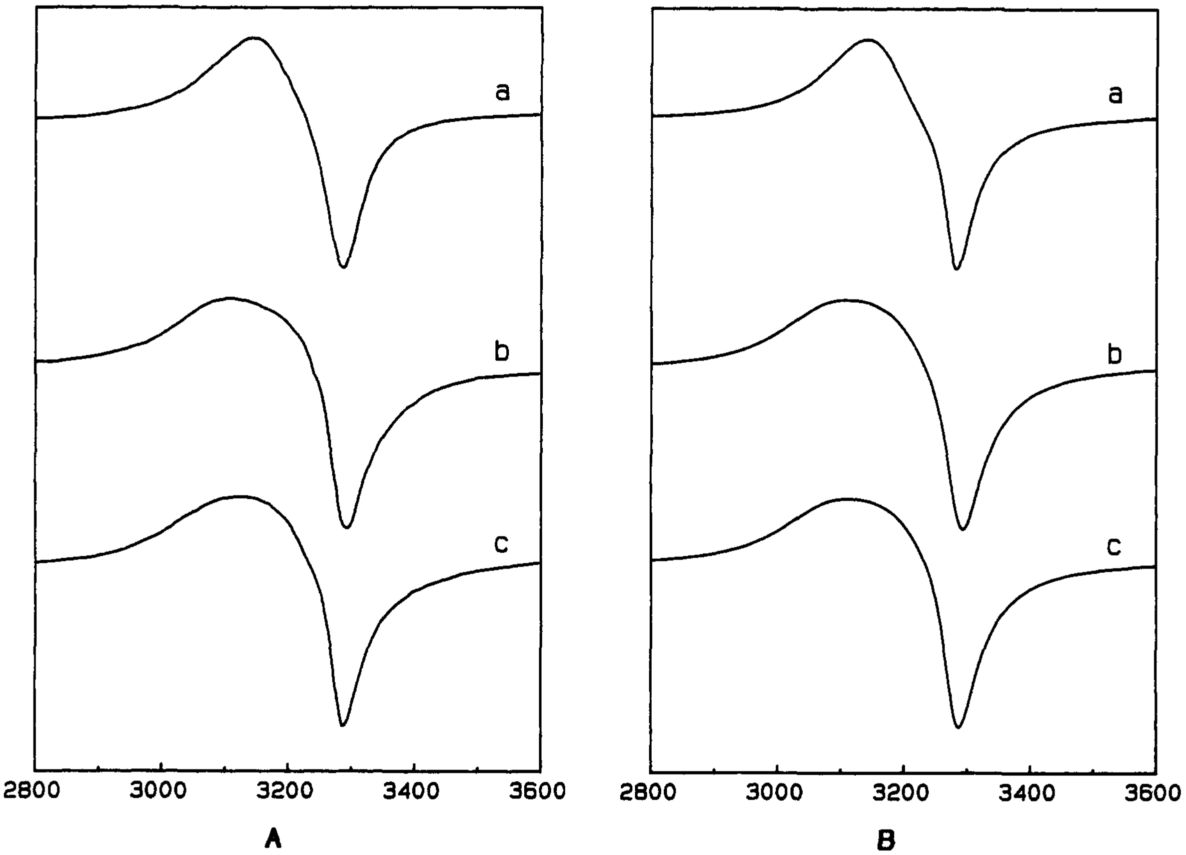

Figure 2. Observed (A) and calculated (B) X-band EPR spectra of $(C_4H_9L)_2Cu$, **4**: a, smectic A phase; b, smectic B phase; c, smectic E phase.

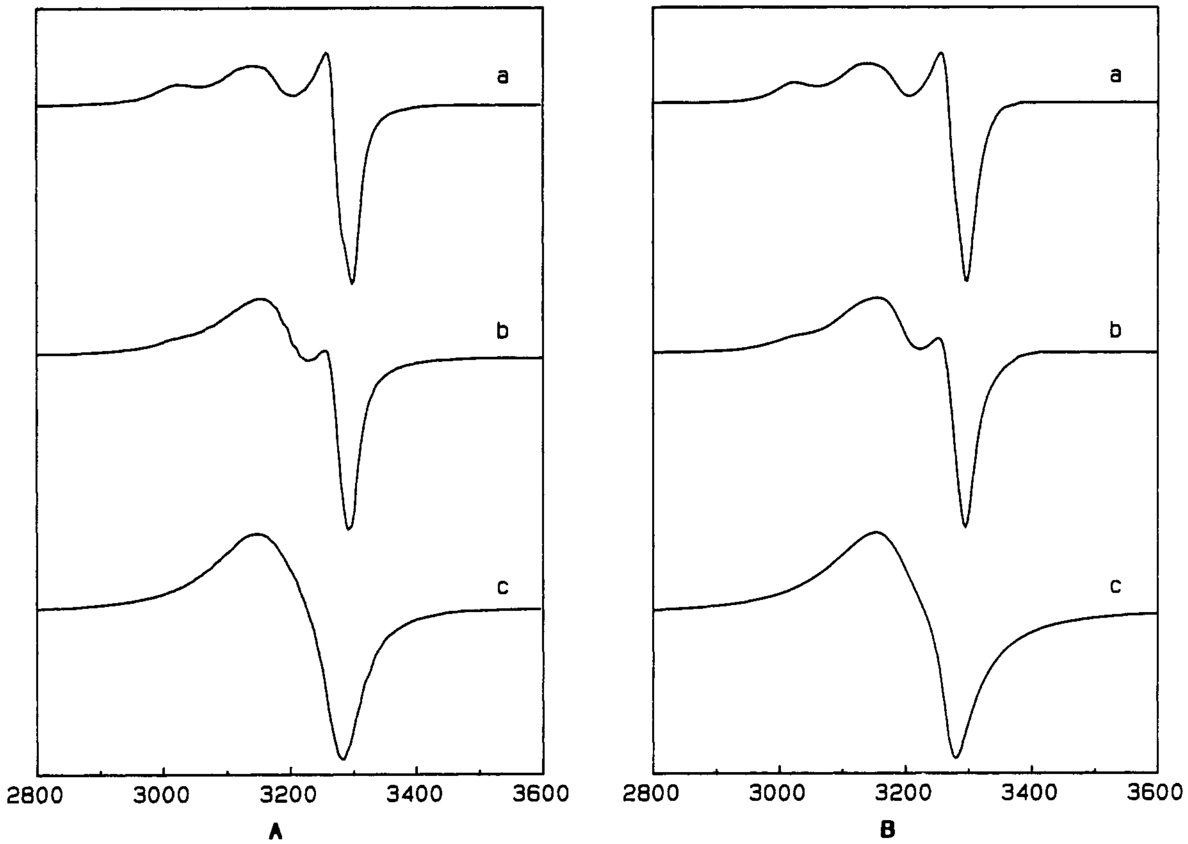

Figure 3. Observed (A) and calculated (B) X-band EPR spectra of $(C_6H_{13}L)_2Cu$, **5**: a, room temperature; b, at 60 °C; c, smectic A phase.

Table III. EPR Spectral Parameters Obtained by the Fit Procedure Described in the Text for the $(R_nL)_2Cu$ Complexes, by Using Lorentzian Line Shapes

compd	type[c]	g_1	g_2	g_3	lw_1	lw_2	lw_3
1	FP	2.167	2.130	2.065	56.0	35.0	15.0
2	FP	2.176	2.103	2.050	45.0	18.0	9.0
2	S_A	2.152	2.086	2.054	50.0	45.0	16.0
3	FP	2.175	2.104	2.047	21.0	11.5	8.0
3	S_A	2.130	2.110	2.055	72.0	50.0	14.0
4A (93%)	FP[a]	2.225	2.060	2.047	22.0	9.0	9.0
4B (7%)	FP[a]	2.220[b]	2.110	2.047	20.0	8.0	8.0
4	S_A	2.145	2.110	2.055	58.0	49.0	13.5
4	S_B	2.190	2.090	2.050	60.0	55.0	18.0
4	S_E	2.190	2.090	2.054	60.0	55.0	16.0
5A (57%)	FP[a]	2.230	2.059	2.042	20.0	8.0	7.5
5B (43%)	FP[a]	2.155	2.113	2.036	25.0	20.0	9.0
5A (38%)	T[a]	2.230	2.059	2.042	30.0	10.0	10.0
5B (62%)	T[a]	2.155	2.109	2.045	35.0	22.0	10.0
5	S_A	2.132	2.115	2.059	80.0	44.0	14.0
6	FP	2.210	2.080	2.046	30.0	16.0	10.5
6	S_A	2.134	2.120	2.059	79.0	39.0	15.5
7	FP	2.230	2.065	2.050	32.0	15.0	10.0

[a] The room-temperature spectra of **4** and **6** and the 60 °C spectrum of **6** were fitted as weighted sum of the A and B spectra, which contributions are indicated by the reported percentages. [b] Due to the small intensity of the spectra, the values of g_1 and g_3 are merely indicative. [c] FP = room-temperature EPR spectra of the freshly prepared compound; T = EPR spectra at 60 °C (only for **5**); S_A = smectic phase A; S_B = smectic phase B; S_E = smectic phase E.

Increasing further the temperature determines a variation in the spectrum up to 118 °C (observed smectic S_A phase) where an asymmetric band, similar to that of the smectic S_A phase of $(C_4H_9L)_2Cu$, is observed (see Figures 3Ac and 2Aa). This feature remains unchanged up to 133 °C, than evolves up to 140 °C to the isotropic liquid spectrum with $g_{av} = 2.09$.

When the samples cool, the spectra broaden slowly and at least two features can be distinguished at 88 °C with $g_\parallel = 2.18$ and $g_\perp = 2.06$. The anisotropy increases on decreasing the temperature, and at room temperature a very broad spectrum is obtained. Low-temperature spectra are similar to the room-temperature spectrum of the fresh sample, with narrower lines.

For all the compounds the room-temperature spectra obtained after a thermal treatment are never equal to those of the freshly prepared compounds, revealing hysteresis effects.

The computer fitting of the spectra of all the compounds according to the procedure reported in the Experimental Section is reported in Table III.

The room-temperature spectra are all well reproduced by using a Lorentzian line shape and appear to be sensitive to the length of the R_n chain, with a decrease of the

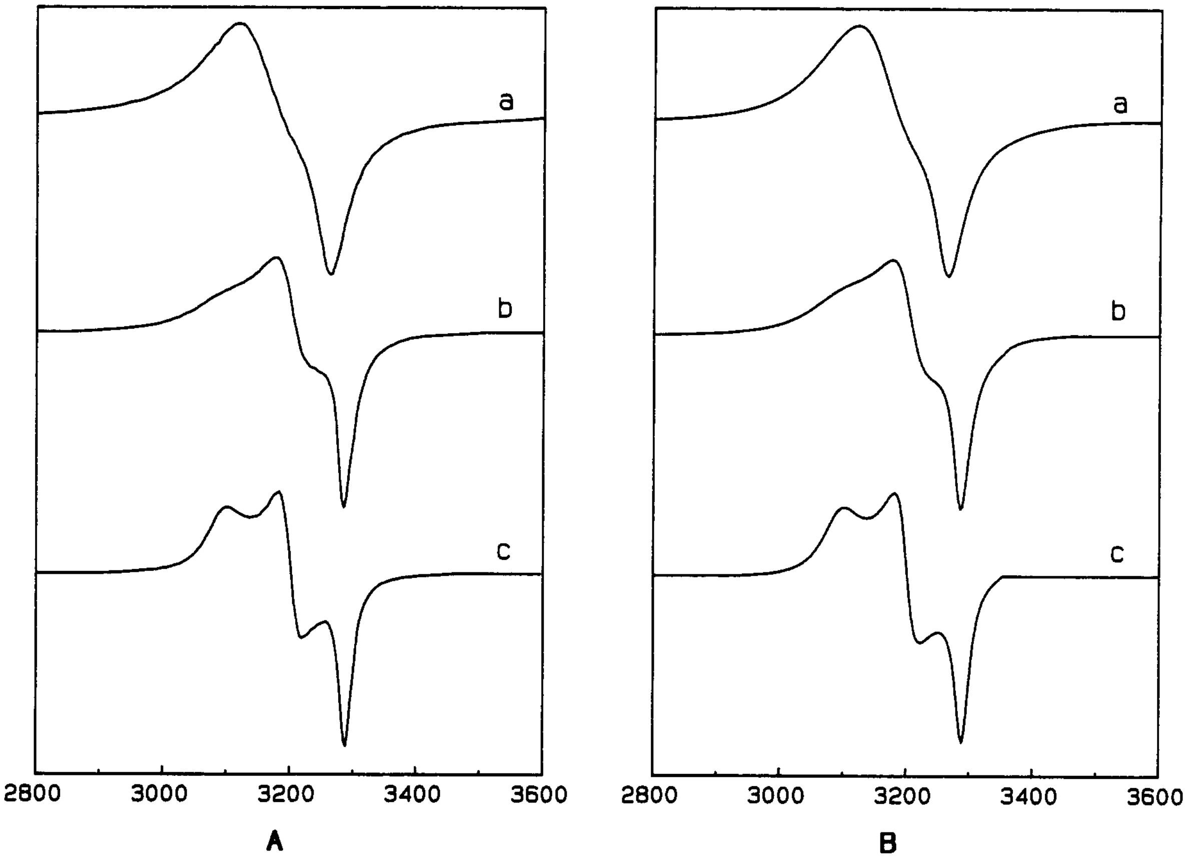

Figure 4. Observed (A) and calculated (B) X-band EPR spectra of $(CH_3L)_2Cu$, **1**; $(C_2H_5L)_2Cu$, **2**; $(C_3H_7L)_2Cu$, **3**.

rhombicity increasing the *n* value (see Figure 4).

For the axial spectra $g_{\parallel} > g_{\perp}$ for all the compounds, and the best-fit results always indicate $\mathrm{lw}_{\parallel} \gg \mathrm{lw}_{\perp}$ (where *lw* are the line widths associated with the *g* values) in agreement with the unresolved hyperfine pattern observed for analogous copper(II) compounds.

Discussion

The investigated $(R_nL)_2Cu$ compounds have the molecular structure depicted in Chart II; therefore, their molecular length should be determined by the contribution due to the two $OC_{12}H_{25}$ aliphatic chains. Space-filling requirements suggested a molecular array formed by interdigitated molecules.[4a] Such a model was successively improved, on the basis of X-ray studies performed on the four shortest terms of this series,[25] which suggested that also the two chains lying on the same side of the complex molecule might be partially folded. As a result, by enlarging the R_n chain the dynamical disorder increases. Morever, the solid phases obtained from the melt were in any case different from the starting crystalline solid. In fact an amorphous phase was found to be present together with a quasi-crystalline ordered phase. The relative amounts of the two phases were found to depend on the thermal history of the samples. The amorphous structure was supposed to be determined by the aliphatic chains which remain trapped in the fork-shaped molecules when the interfaces between different layers freeze and the solid phase forms.[25]

Such a packing mode is confirmed by the EPR measurements. In fact, the room-temperature spectra also depend on the thermal hystory of the sample, and in particular the two distinct spectra, A and B, exhibited by both **4** and **5** can be assigned to the quasi-crystalline and the amorphous structures, respectively. This interpretation agrees also with the variation of the relative intensities of the two spectra on increasing temperature. In fact, since for a given solid it was found that the degree of crystallinity decreases as the temperature increases,[25] both the higher intensity of the spectrum of the **5B** species upon heating and the disappearance of the **4B** spectra on cooling agree with this model.

The molecular geometry sketched in Chart II for all the present compounds suggests axial spectra with $g_{\parallel} \approx 2.2$ and $g_{\perp} \approx 2.05$ as previously observed for other copper(II) complexes with Schiff bases.[28,34-37] The room-temperature spectra of **4A**, **5A**, **6**, and **7** conform to thise scheme, while **1**–**3** show large rhombic anisotropies (see Figure 4). The common feature of the spectra of **1**–**3** is that the lowest *g* value, g_3, is close to $g_{\perp}$ observed in copper(II) Schiff base complexes and also to $g_{\perp}$ in **4**–**7**, while g_1 and g_2 are between the $g_{\parallel}$ and $g_{\perp}$ values. Patterns of *g* values like those exhibited by **1**–**3** are well-known in the EPR spectra of copper(II) compounds, and they have always been found to originate from partial averaging of $g_{\parallel}$ and $g_{\perp}$ signals.[38,39]

In priniciple largely rhombic *g* values might also have a molecular origin,[40,41] but this is expected only for five-coordinate complexes with geometry intermediate between square pyramid and trigonal bipyramid, which can be ruled out in the present case.

---

(34) Wasson, J. R.; Cowan, P. J.; Hatfield, W. E. *Inorg. Chim. Acta* **1978**, *27*, 167.

(35) Lancione, R. L.; Allen, H. C., Jr.; Sydor, D. R. *J. Coord. Chem.* **1975**, *4*, 153.

(36) Lancione, R. L.; Allen, H. C., Jr. *J. Coord. Chem.* **1975**, *4*, 261.

(37) Scullane, M. I.; Allen, H. C., Jr. *J. Coord. Chem.* **1975**, *4*, 255.

(38) Bencini, A.; Gatteschi, D. *Transition Met. Chem. (N.Y.)* **1982**, *8*, 1.

(39) Bertini, I.; Gatteschi, D.; Scozzafava, A. *Coord. Chem. Rev.* **1979**, *29*, 64.

(40) Bencini, A.; Bertini, I.; Gatteschi, D.; Scozzafava, A. *Inorg. Chem.* **1978**, *17*, 3194.

(41) Wasson, J. R.; Klassen, D. M.; Richardson, H. W.; Hatfield, W. E. *Inorg. Chem.* **1977**, *16*, 1906.

Scheme II. Possible Scheme of the Molecular Array That Leads to the Intermolecular Averagig Process Observed for the Solid Phases

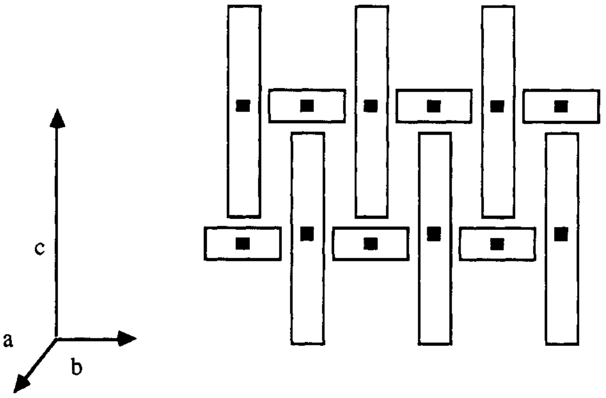

In general the averaging process has been observed to have an intermolecular origin[38,39] mediated by exchange interactions. This occurs when tetragonally distorted copper(II) complexes orient with the *z* axis of one molecule parallel to the *x* axis of another molecule and intermolecular exchange interactions average the two signals. A possible scheme for this averaging process for the present compounds is shown in Scheme II: axial and equatorial positions alternate in the *bc* plane, while orthogonal to the plane all the molecules have equatorial positions and $g = g_\perp$.

However this arrangement is completely different from that of Scheme I, which was supported by X-ray evidence. Further, the arrangement of Scheme I is confirmed also by the single-crystal X-ray analysis[29] of bis[*N*-4-(*n*-hexyloxy)phenyl-4′-(*n*-heptyloxy)salicylaldiminato]copper(II), a mesogenic complex whose molecular structure is similar to that of the $(R_nL)_2Cu$ compounds. Remarkably, such a thermotropic species, which upon heating gives smectic S_C and S_A phases, exhibits a crystal packing formed by layers of molecules; therefore, it seems reasonable to suppose a similar arrangement in the present case too.

On the basis of these considerations we suggest that the observed rhombic *g* values must be interpreted in terms of intramolecular anisotropic motional averaging. If we assume that the molecules can easily rotate around the long molecular axis, they would exchange rapidly $g_\parallel$ with $g_\perp$, keeping the other $g_\perp$ direction constant. A similar mechanism of partially hindered molecular rotation has been suggested on the basis of quasi-elastic neutron scattering studies.[42]

The room temperature EPR spectra of the $(R_nL)_2Cu$ series of sensitive to the length of the R_n chain, with a decrease of the rhombicity increasing the *n* value. In the hypothesis of a layered structure this indicates that a better alignment is progressively achieved on increasing R_n. The rationale for this is the reduction of the difference between the R_n and the $C_{12}H_{25}O$ chains (Chart II), which makes more ordered molecular packings easier.

The $(R_nL)_2Cu$ complexes exhibit one or more smectic phases including a S_A phase (Table II), whose EPR spectra is characterized by a line shape independent of the length of the R_n chain.

A previously reported study on orientationally ordered smectic copper metal complexes films[43,44] evidenced polydomains structures with a strong monoaxial orientation orthogonal to the film plane and a random distribution of the other two principal axes in the film plane. The EPR spectra of such systems appear to be determined by the superposition of the spectra of all the domains. In our case, where no attempt to obtain homeotropic orientation of the smectic phases was done, the random distributions of the domains in the samples result in powderlike EPR spectra. We fit the EPR spectra of the smectic phases using a rigid model, whose validity in the present case is justified by the above consideration and by the high-viscosity of the systems far from the melting point. Table III shows that the *g* values and the line widths for the S_A phases are practically equal to each other, independent of the compound and of its thermal behavior. The smectic S_A phase for this class of compounds is then clearly distinguishable by EPR and exhibites rhombic spectra with $2.13 < g_1 < 2.15$, $2.10 < g_2 < 2.12$, and $2.05 < g_3 < 2.06$. From Table III it can be observed that the EPR spectra of the S_A smectic phases have larger line widths and smaller $|g_1 - g_2|$ with respect to the room-temperature spectra.

The smectic S_E phase is observed only for the $(C_4H_9L)_2Cu$ and for the $(C_6H_{13}OL)_2Cu$: its spectrum is independent of the compound and can be fitted with a slightly more rhombic *g* tensor than that of the S_A phase (Table III) and a Lorentzian line shape. The smectic S_B phase is exhibited only by $(C_4H_9L)_2Cu$, and its EPR spectral results are practically indistinguishable from those of the S_E phase. On the basis of the above consideration, it can be deduced that the formation of the smectic S_A phases is accompanied by a disordering in the structure of the compounds with an increase in the misalignement in the principal directions of the molecular **g** tensor.

Concluding, the results arising from the present investigation, together with a confirmation of the molecular packing previously proposed on the basis of the X-ray investigations,[25] show that the smectic S_A phase gives rise to a peculiar EPR line shape, which, in the system under study, can be used to individuate it.

Acknowledgment. This work was supported by the Italian Consiglio Nazionale delle Ricerche (CNR) under the cover of "Progetto Finalizzato Materiali Speciali per Tecnologie Avanzate".

---

(42) Rustichelli, F.; Pagnotta, M. C.; Versace, C.; Ghedini, M.; Armentano, S.; Bartolino, R.; Ricci, M. A. Submitted to *Solid State Commun.*

(43) Galimov, R. M.; Vikchantaav, I. G.; Ovchinnikov, I. V.; Kostantinov, V. N. *Zh. Strukt. Khim.* **1989**, *30*, 59.

(44) Galimov, R. M.; Vikchantaav, I. G.; Ovchinnikov, I. V. *Zh. Strukt. Khim.* **1989**, *30*, 65.